

NUCLEAR STRUCTURE OF $^{15,16}\text{C}$ VIA REACTION
CROSS-SECTION MEASUREMENTS*

H. DU^a, M. FUKUDA^a, D. NISHIMURA^b, M. TAKECHI^c, T. SUZUKI^d
Y. TANAKA^a, I. KATO^d, M. TANAKA^a, K. ABE^b, T. IZUMIKAWA^e
H. OIKAWA^b, T. OHTSUBO^c, J. OHNO^a, Y. KANKE^b, H. KIKUCHI^c
A. KITAGAWA^f, S. SATO^f, U. SAYAMA^c, J. SHIMAYA^a, S. SUZUKI^g
Y. TAKEUCHI^d, T. TAKEMOTO^b, N. TADANO^d, R. TAMURA^b
J. NAGUMO^b, K. NISHIZUKA^c, S. FUKUDA^f, K. HORI^b
S. MATSUNAGA^d, A. MIZUKAMI^b, M. MIHARA^a, E. MIYATA^c
D. MUROOKA^c, S. YAMAOKA^a, T. YAMAGUCHI^d

^aDept. Physics, Osaka University, Toyonaka, Osaka 560-0043, Japan

^bDept. Physics, Tokyo University of Science, Chiba 278-8510, Japan

^cDept. Physics, Niigata University, Niigata 950-2181, Japan

^dDept. Physics, Saitama University, Saitama 338-3570, Japan

^eRadioisotope Center, Niigata University, Niigata 951-8510, Japan

^fNational Institute of Radiological Sciences, Chiba 263-8555, Japan

^gDept. Physics, Tsukuba University, Ibaraki 305-8577, Japan

(Received December 14, 2016)

Reaction cross sections for $^{15,16}\text{C}$ on nuclear targets (Be, C, Al) and proton target are systematically measured in the intermediate energy range. Nucleon density distributions of $^{15,16}\text{C}$ were deduced from the analyses of present data with existing experimental data using the Glauber-type calculation. Proton and neutron density distributions were also deduced separately from proton target data. Results of root-mean-square radii show a good agreement with theoretical calculations for both isotopes.

DOI:10.5506/APhysPolB.48.473

1. Introduction

Radius or nucleon density is one of the fundamental properties of nuclei. Such attributes of unstable nuclei can be significantly different from ones of stable nuclei. In an unstable region, unique nuclear structures such as halo and skin structure are observed. Since the number of unstable nuclei is exceedingly large, it is important and intriguing to probe and quantitatively discuss their nucleon density distributions.

* Presented at the Zakopane Conference on Nuclear Physics “Extremes of the Nuclear Landscape”, Zakopane, Poland, August 28–September 4, 2016.

^{15}C is an unstable neutron-rich carbon isotope, with small one-neutron separation energy, $S_n = 1.218$ MeV [1]. It plays an important role in the following hot-CNO cycle that is considered to take place in asymptotic giant branch (AGB) stars



This chain reaction is triggered by the neutron capture of ^{14}C , the possibility of which depends on nuclear structure of ^{15}C . In a neutron-rich environment, $^{15}\text{C}(n, \gamma)^{16}\text{C}$ reaction can work against the chain reaction if the nuclear structure of ^{16}C allows. Thus, by studying the nuclear structure of $^{15,16}\text{C}$, we can have a better understanding of galactic evolution and synthesis of heavier elements.

Several studies regarding ^{15}C have pointed out the evidence of halo structure, such as Bazin's research on momentum distributions of ^{14}C in $1n$ knock out reaction of ^{15}C [2], and more recently, Nakamura's study on the Coulomb break-up reaction [3]. Measurements of reaction cross sections (σ_R) also remain a powerful tool of probing nuclear densities and radii. The σ_R for $^{15,16}\text{C}$ on nuclear targets were measured at several energies in the previous studies [4–7], however, not yet adequate enough to assert the density distributions.

In this research, we systematically measured σ_R for $^{15,16}\text{C}$ in the intermediate energy range, which is very sensitive to reactions taking place near the surface of nuclei. The experimental method will be described in detail in Section 2. In Section 3, the preliminary results will be discussed.

2. Experiment

The experiment was carried out in the National Institute of Radiological Sciences, Japan, using the heavy-ion synchrotron facility HIMAC. In order to produce $^{15,16}\text{C}$ beams with several energy ranged in between 40–140 MeV/nucleon, projectile fragmentation of 200 MeV/nucleon ^{18}O primary beam on Be production targets was used. Isotopes in secondary beams were separated by the fragment separator consisting of two dipole magnets and an Al wedge degrader.

In addition to the initial separation by the separator, particles were identified by the $B\rho$ -TOF- ΔE method before reaching the reaction target. After reaction target, the outgoing particles were identified by a ΔE - E counter telescope, which was placed closely at down stream of reaction targets to ensure a large solid angle detection.

The σ_R are measured by the transmission method. Through particle identification, the number of incoming projectile before the target (N_0) and the number of outgoing non-reacted particles after the target (N_1)

are counted. Measurements without reaction targets were also performed to make corrections for reactions in the detectors. Thus, σ_{R} can be deduced by the following equation, where t is the thickness of reaction target, $R_{\text{in}} = N_1^{\text{in}}/N_0^{\text{in}}$ ($R_{\text{out}} = N_1^{\text{out}}/N_0^{\text{out}}$) is the non-reaction rate with (without) the reaction target

$$\sigma_{\text{R}} = -\frac{1}{t} \ln \left(\frac{R_{\text{in}}}{R_{\text{out}}} \right). \quad (1)$$

High purity Be, C, Al are employed as the nuclear targets. In addition, measurements of σ_{R} on CH_2 targets were also performed. The σ_{R} on proton targets can be derived by the following equation:

$$\sigma_{\text{R}}^p = -\frac{\sigma_{\text{R}}^{\text{CH}_2} - \sigma_{\text{R}}^{\text{C}}}{2}. \quad (2)$$

3. Results and discussions

3.1. Result for ^{15}C

σ_{R} measured for ^{15}C are plotted against the average energy of beams in the target in Fig. 1 (a). The σ_{R} data measured at intermediate energies (51

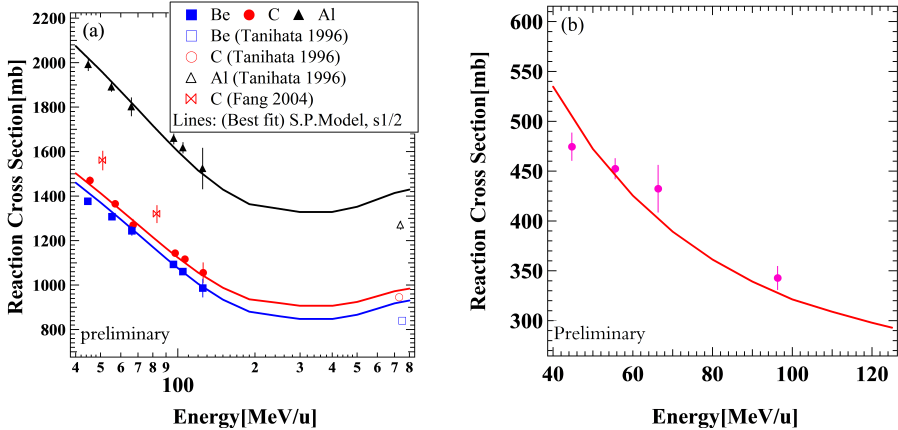


Fig. 1. (Color online) (a) The full markers represent σ_{R} for ^{15}C measured by the present experiment, on Be (square/blue), C (circle/red) and Al (triangle/black) targets. Open markers at 740 MeV/u represent previous measurements of Tanihata *et al.* [4]. Data Points at intermediate energies (51 and 83 MeV/u) are referred to the data of Fang *et al.* [5]. Solid lines are the best-fit result of present value by the modified Glauber type calculations, in which a single-particle model with a valence neutron in $2s_{1/2}$ orbital is assumed. (b) Full markers are the present σ_{R}^p data for ^{15}C (on proton targets), the solid line is the best-fit result.

and 83 MeV/ u) by Fang *et al.* [5, 6] and at 730 to 750 MeV/ u by Tanihata *et al.* [4] are also plotted. Figure 1 (b) shows the present σ_R^p (on proton) data deduced from Eq. (2).

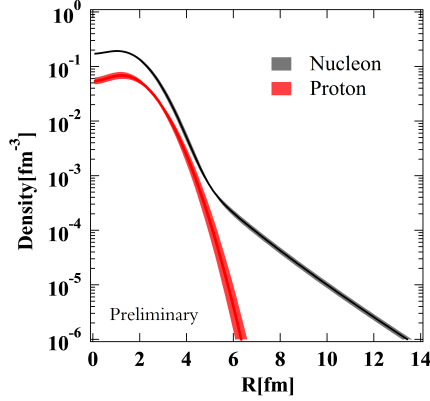


Fig. 2. (Color online) Density distributions of ^{15}C : Nucleon density distribution (darker/gray line) deduced from σ_R on nuclear targets, with shaded area representing the error. Lighter/red line and shaded area represents the proton density distribution and its error, deduced from σ_R on proton targets. The difference between them is the neutron density. A large tail of neutron is observed.

The σ_R can be predicted for an assumed density distribution by the modified Glauber type calculation introduced by Takechi *et al.* [8]. This calculation can precisely reproduce σ_R for not only stable nuclei, but also for unstable nuclei with reliably known density distributions. In the present study, calculations with different models for density distribution were used in the analyses of the present σ_R data. The best model we found is a single-particle model, with Harmonic-Oscillator-type (HO) ^{14}C core and one weakly bound valence neutron occupying $2s_{1/2}$ orbital, the binding energy of which is the experimental value $S_n = 1.218$ MeV. The width of the core and amplitude of the single-particle density are free parameters in the fitting to reproduce the measured σ_R . This best-fit result is also shown in Fig. 1 with solid lines. The best-fit nucleon density distribution ρ_N is plotted in Fig. 2 by the darker/gray line. The shaded area represents the fitting error.

Next, we assumed the proton density distribution ρ_p to be of HO-type, thus a neutron density distribution can be derived by $\rho_n = \rho_N - \rho_p$. By changing the width of proton density and applying corresponding ρ_p and ρ_n pairs to the Glauber calculation, the best density distribution that fits experimental data σ_R^p can be deduced. The solid line in Fig. 1 (b) is the best-fit result, while the deduced proton density is shown in Fig. 2 with the lighter/red line, shaded area represents the error. A large tail of neutrons is observed in the nucleon density distribution of ^{15}C .

3.2. Result for ^{16}C

The measured σ_R for ^{16}C are plotted against average energies in Fig. 3 (a). The σ_R data at intermediate energies (39 and 83 MeV/u) are experimental values by Fang *et al.* [5, 6] and Zheng *et al.* [7]. Measured data at 790 MeV/u by Tanihata *et al.* [4] are also plotted. Figure 3 (b) shows the present σ_R^p data. Solid lines are the best-fit results. For ^{16}C , we also included the mixture percentage of valence neutron's orbital as a fitting parameter. The best model to reproduce the experimental value is a single-particle model, with a ^{14}C core and two valence neutrons occupying a mixture of 50% $2s_{1/2}$ orbital and 50% $1d_{5/2}$ orbital, the binding energy of this system is two-neutron separation energy of ^{16}C .

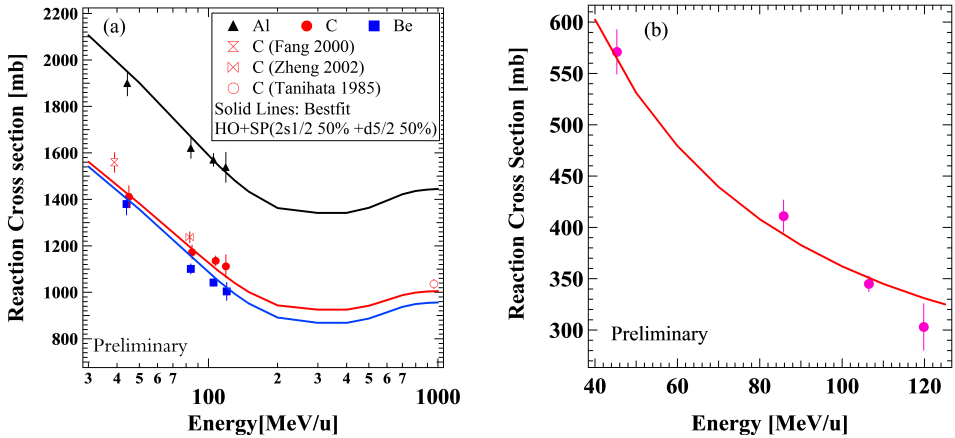


Fig. 3. (Color online) (a) The full markers represent σ_R for ^{16}C measured by the present experiment, on Be (square/blue), C (circle/red) and Al (triangle/black) targets. Open markers at 790 MeV/u represent previous measurements of Tanihata *et al.* [4]. Data Points at intermediate energy range (39 and 83 MeV/u) are referred to the data of Fang *et al.* [6] and Zheng *et al.* [7]. Solid lines are the best-fit result by the modified Glauber type calculations. (b) Full markers are the present σ_R^H data for ^{16}C (on proton targets), solid line is the best-fit result.

The ρ_p and ρ_n are also deduced separately. Figure 4 shows the nucleon (proton) density distribution with lighter gray (darker red) line, shaded areas are the errors. A tail can be seen in the neutron density distribution, however it is not as extended as ^{15}C .

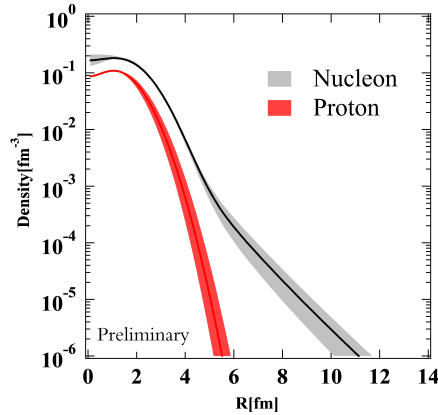


Fig. 4. (Color online) Density distributions of ^{16}C : Nucleon density distribution (lighter/gray line) deduced from σ_R on nuclear targets, where shade area represents the error. Darker/red line and shade area represent proton density distribution and its error, deduced from σ_R on proton targets. The difference between them is the neutron density.

3.3. Root-mean-square (RMS) radii

RMS radii of nucleon, proton and neutron distributions for $^{14,15,16}\text{C}$ are deduced from the present density distributions are shown in Fig. 5 by solid markers. Data of ^{14}C are analyzed by Kato *et al.* [13]. Proton radii deduced

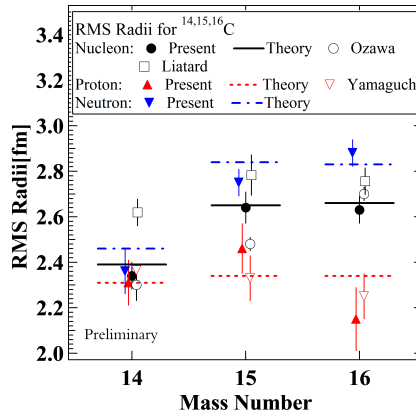


Fig. 5. Full markers represent the present data, RMS radii of nucleon (circle), proton (triangle) and neutron (inverted triangle) distributions for $^{14,15,16}\text{C}$. Open circles are referred to Ozawa *et al.* [9]. Open squares are referred to Liatard *et al.* [12]. Open inverted triangles are the proton RMS radii measured by Yamaguchi *et al.* [10]. Theoretical calculations by Abu-Ibrahim *et al.* [11] are also plotted with lines.

by Yamaguchi *et al.* [10] from charge changing cross sections are also plotted. Within the error range, present data are in agreement with referred proton radii. Nucleon radii from Liatard and Ozawa *et al.* [9, 12] are also plotted. Present data show better agreement with theoretical work by Abu-Ibrahim *et al.* [11], which are also plotted in Fig. 5.

4. Summary

We have studied the nuclear structure of $^{15,16}\text{C}$ by systematic measurements of reaction cross sections on nuclear targets (Be, C, Al) and proton target in the intermediate energy range. For ^{15}C , a single-particle model with a Harmonic-Oscillator-type (HO) ^{14}C core and one weakly bound valence neutron occupying $2s_{1/2}$ orbital reproduced present data very well. For ^{16}C , the best model to reproduce experimental value is also a single-particle model with the ^{14}C core and two valence neutrons occupying a mixture of 50% $2s_{1/2}$ orbital and 50% $1d_{5/2}$ orbital, assuming the binding energy of one valence neutron is a half of the two-neutron separation energy of ^{16}C . The best-fit nucleon density distributions of $^{15,16}\text{C}$ were deduced from the analyses of present data with existing experimental data using the Glauber type calculation. Proton and neutron density distributions were also deduced separately from proton target data. In the density distributions of ^{15}C , a large neutron tail can be observed, which suggests a halo structure. This conclusion is consistent with recent studies [2, 3, 5]. A neutron tail is also seen in the neutron density distribution of ^{16}C , however not as extended as ^{15}C . Results of root-mean-square radii show a good agreement with theoretical calculations for both isotopes [11].

REFERENCES

- [1] G. Audi, A.H. Wapstra, *Nucl. Phys. A* **565**, 66 (1993).
- [2] D. Bazin *et al.*, *Phys. Rev. C* **57**, 2156 (1998).
- [3] T. Nakamura *et al.*, *Phys. Rev. C* **79**, 035805 (2009).
- [4] I. Tanihata *et al.*, *Phys. Lett. B* **160**, 380 (1985).
- [5] D.Q. Fang *et al.*, *Phys. Rev. C* **69**, 034613 (2004).
- [6] D.Q. Fang *et al.*, *Phys. Rev. C* **61**, 064311 (2000).
- [7] T. Zheng *et al.*, *Nucl. Phys. A* **709**, 103 (2002).
- [8] M. Takechi *et al.*, *Phys. Rev. C* **79**, 061601 (2009).
- [9] A. Ozawa *et al.*, *Nucl. Phys. A* **693**, 32 (2001).
- [10] T. Yamaguchi *et al.*, *Phys. Rev. Lett.* **107**, 032502 (2011).
- [11] B. Abu-Ibrahim, W. Horiuchi *et al.*, *Phys. Rev. C* **77**, 034607 (2008) [*Errata ibid.* **80**, 029903 (2009), **81**, 019901 (2010)].
- [12] E. Liatard *et al.*, *Europhys. Lett.* **13**, 401 (1990).
- [13] I. Kato *et al.*, private communication.